

## LEAD FREE METALLISATION FOR SILICON SOLAR CELLS: RESULTS FROM THE EC2CONTACT PROJECT

Jaap Hoornstra<sup>1</sup>, Gunnar Schubert<sup>2</sup>, Cécile LePrince<sup>3</sup>, Gerhard Wahl<sup>4</sup>  
Kees Broek<sup>1</sup>, Filip Granek<sup>1</sup>, Beate Lenkeit<sup>4</sup>, Jörg Horzel<sup>5</sup>

<sup>1</sup>ECN Solar Energy, PO Box 1, 1755 ZG Petten, the Netherlands, p:+31.224.564697, hoornstra@ecn.nl

<sup>2</sup>University of Konstanz, PO Box X916, 78457 Konstanz, Germany, p:+49.7531.88.2088, gunnar.schubert@uni-konstanz.de

<sup>3</sup>Metalor Technologies, 45 Rue de Paris, 93130 Noisy-le-Sec, France, p:+33.148.50.5547, cecile.leprince@metalor.com

<sup>4</sup>RWE Schott Solar, Theresienstrasse 2, 74072 Heilbronn, Germany, p:+49.7131.67.2683, gerhard.wahl@rweschottolar.com

<sup>5</sup>RWE Schott Solar, Carl-Zeiss-Strasse 4, 63755 Alzenau, Germany, p:+49.6023.91.1735, joerg.horzel@rweschottolar.com

**ABSTRACT:** This paper reports the successful development of lead free thick film metallisation pastes for contacting crystalline silicon solar cells, as performed in the EC2Contact project. Due to detailed characterization, we now understand the process of contact formation of front side metallisation pastes to silicon. New test procedures have reduced the number of experiments. Silver pastes with lead free glass frits were formulated on basis of the contact model and tested using the new approaches. Cells were produced on texturized Cz crystalline silicon and SiN<sub>x</sub> anti reflection coating. Using the best lead free silver front side paste, a fill factor of 77.2% and efficiency of 17.0% was reached, equal to results from a reference paste using leaded frit. The best rear side aluminium paste with lead free frit performed similar as compared to the reference aluminium paste with 76.5% FF and 17.1% efficiency.

**Keywords:** lead free, paste, cSi, metallisation, screen printing

### 1 INTRODUCTION

From January 2002, a European consortium of the above mentioned institutes worked on a three-year R&D-project called "EC2Contact", funded by the European Commission in the 5<sup>th</sup> Framework Programme [1]. The aim of the project was to develop environmentally benign metallisation for crystalline silicon solar cells.

The electronic industries are demanded for several years to work with environmentally clean materials. The EU "RoHS-directive" (restriction of use of certain hazardous substances) regulates that from July 2006 electrical and electronic equipment put on the market may not contain lead above a maximum concentration value of 0.1% by weight in homogeneous materials. Currently this directive is not applicable to PV modules. Awareness on these matters, however, exists in the PV world as is reflected by the work of Tsuo [2] in 1998, and more recently, of de Wild [3, 4]. Some manufacturers already anticipate similar regulations for PV products and advertise the use of lead free materials, accounting for e.g. lead free soldering or glass frit free rear side paste. In general, however, pastes with lead containing glass frits are used to produce the electrical contacts.

The goal of the work reported here is to find in an intelligent and effective way a replacement for the lead in glass frit and to obtain at least competitive cell results with these lead free pastes. Our approach was to understand and model the mechanisms of contact formation and current transport in order to determine the role of the lead. To effectively decrease the number of experimental testing, new experimental test procedures were developed and used.

The work on the *contact formation model* is described below, followed by a chapter dealing with *experiments on paste performance* to assess the performance of the developed frits and pastes on cell level. In the final chapter the best *results* are given.

### 2 CONTACT FORMATION MODEL AND ASSOCIATED EXPERIMENTS

#### 2.1 Approach

Our approach to develop lead free front side pastes was to firstly understand the contact formation and current transport mechanism of successful lead containing silver pastes. The competing processes were investigated separately, with focus on the role of glass frit, and especially on the role of lead oxide, in order to find a substitution for this oxide.

The contact formation was studied in detail using SEM, EDX, DTA and XRD. Additionally new approaches, such as in-situ contact resistance measurements, were developed and used [5]. Most of the experiments were performed in an RTP furnace (Steag AST - SHS 100), providing accurate temperature control of the sample during firing. For maximum flexibility in the choice of constituents, glass frits were fabricated and their viscosity-temperature, wetting and etching behaviour investigated.

It was found that the glass frit plays the most important role during contact formation. Its task is not only to etch through the antireflection coating and to ensure a stable mechanical contact. Additionally the glass serves as a transport medium for silver to grow preferentially on <111> oriented silicon planes. It ensures the formation of nearly perfect silver-silicon contacts at temperatures below the silver-silicon eutectic. Various experiments with silver pastes and designed silver-glass-silicon systems were performed to study the silver transport and growth process in detail [5]. The results led to a detailed model of contact formation.

#### 2.2 Contact formation model with leaded glass frit

At temperatures typically above 600°C glass frit particles get fluid, wet and start to etch the SiN<sub>x</sub>. As soon as the glass has penetrated the dielectric layer, etching into silicon occurs via a redox reaction between lead oxide and silicon [6]. The resulting metallic lead is liquid in this stage of the firing process. As soon as liquid lead comes into contact with silver the silver particles melt to form a liquid silver-lead phase according to the silver-lead phase diagram. The silver-lead melt seems to

dissolve <100> silicon planes, so that inverted pyramids are formed. On cooling down, silver and lead separate according to their phase diagram. Consequently silver recrystallizes on the <111> planes of the inverted pyramid. Lead is therefore assumed to be the transport medium for silver to grow onto the silicon. Recently it was found that the number and size of the grown silver crystals depend on the surface phosphorous concentration of the emitter [7].

Even though the dominant current transport mechanism in thick film silver contacts is not identified yet, the silver crystallites seem to be indispensable to establish an effective current path from the emitter into the bulk of the thick film finger. The contact resistivity between silicon and silver crystals was measured to be in the range of  $0.2 \mu\text{Ohmcm}^2$  on highly doped emitters [8]. Most of the crystals are separated from the bulk of the silver finger by a shallow glass layer, therefore the glass frit also plays a role in the current transport [9]. The tunnelling probability through the layer might be increased due to the chemical modification of the glass during the firing process.

Following this contact formation model it seems to be essential for a lead free glass to contain metal oxides that are reduced by silicon in the relevant temperature regime. The resulting metal should form an alloy with silver that interacts with silicon in a way that an almost perfect metal-semiconductor contact is formed.

### 2.3 Study on lead oxide replacements

To find the best lead free glass frit several metal oxides were analysed and tested. Pastes were produced of silver powder and the metal oxide (MO) to be studied. According to the contact formation model described above the metal should serve as a transport medium for silver to grow on silicon. In Figure 1 the silicon surface after removing the MO + Ag paste of the best performing metal is shown. Silver crystals grown on the silicon are clearly visible.

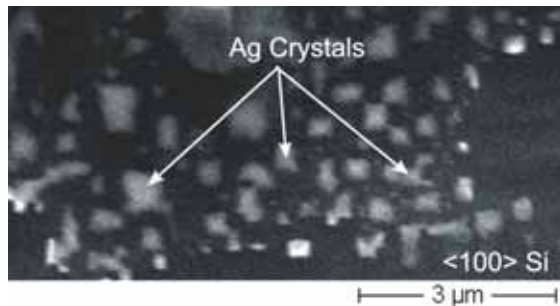
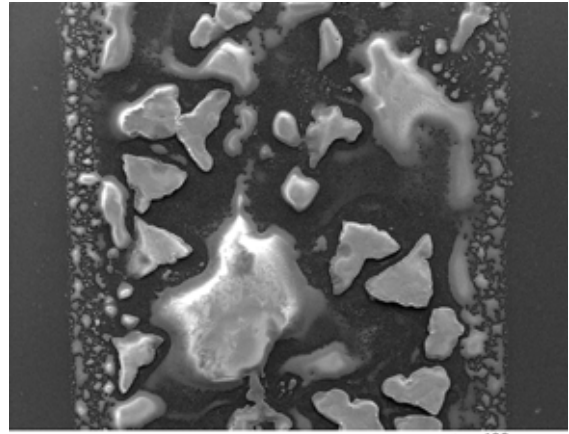


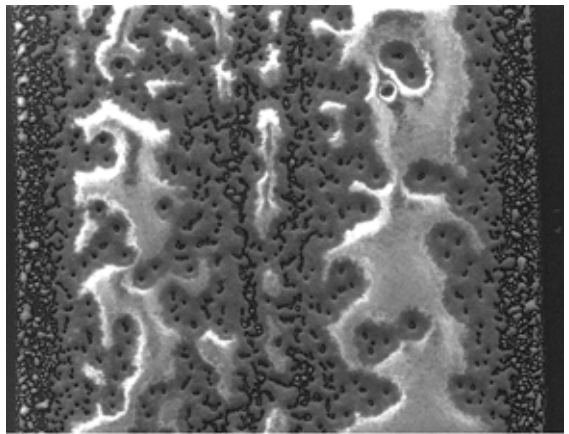
**Figure 1:** SEM picture of <100> silicon surface below the MO + Ag paste after removing the paste, showing the Ag crystals grown in the inverted pyramids. The sample was fired at 800°C for 2 min.

The most promising metal oxides served as the basis for fabricating several silicate glasses varying in metal oxide species and content. The essential properties of these frits were tested and evaluated by investigating for example the glass transition temperature using DTA, the etching ability and the wetting behaviour. As an example in Figure 2 the wetting behaviour of two different lead free frits is shown. The main metal oxide is the same but the composition of the frits was varied. For this experiment pastes were prepared containing only glass

frit and an organic binder. Two fingers of each paste were syringe-printed on one sample per temperature (<100> p-type Cz silicon, chemically polished) and investigated using SEM and a surface profiler. From the SEM photographs it can be clearly seen that frit B wets silicon better than frit A.



(a) Frit A



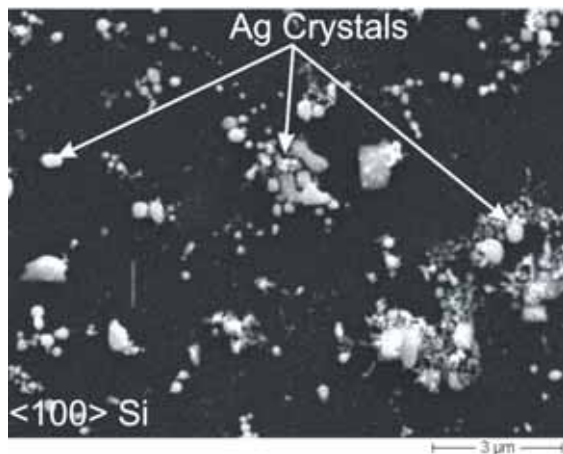
(b) Frit B

**Figure 2:** Comparison of the wetting behaviour of two lead free glass frits. The glass frit pastes were fired on the same <100> Si sample at 800°C ( $t_{\text{peak}} = 0\text{s}$ ).

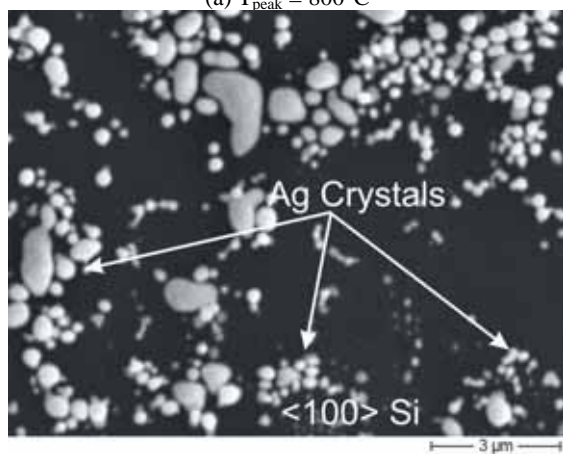
### 2.4 Basic lead free paste experiments

The best glass frits were used to fabricate thick film silver pastes to test the paste performance on cell level. Additionally the silver transfer process to grow on silicon was studied. In Figure 3 the temperature dependence of the silver transfer process of a lead free silver thick film paste is presented. The SEM pictures show the <100> oriented silicon surface after removal of the fingers. Number and size of the silver crystals increase with increasing temperature.

With these tests it was demonstrated that the silver transfer process to the silicon could be done successful with a lead free glass frit. It was shown that a lead free glass frit containing appropriate metal oxides provides the key properties for establishing an electrical contact to the emitter.



(a)  $T_{\text{peak}} = 800^{\circ}\text{C}$



(b)  $T_{\text{peak}} = 850^{\circ}\text{C}$

**Figure 3:** SEM photographs of  $\langle 100 \rangle$  Si surfaces (FZ, chemically polished, 38 Ohm/sq. emitter) after removal of the silver fingers. Silver crystals are clearly visible (white), number and size increase with increasing temperature ( $t_{\text{peak}}: 0.5\text{s}$ )

### 3 EXPERIMENTS ON PASTE PERFORMANCE

#### 3.1 Basic procedure

Based on results from the modelling and associated experiments, various lead free glass frit based silver pastes were made and tested. Also, aluminium pastes were formulated using the found glass frits. Cells were made of 300 micron thick texturized Cz wafers with a  $\text{SiN}_x$  anti reflection coating. For comparison the best performing commercial pastes, containing leaded glass frits, were used. Cells were processed using screen printing and IR belt furnace co-firing, and analysed in detail on IV, Suns-Voc FF, line resistance, contact resistance, finger definition and bowing.

#### 3.2 Temperature profiling and cross belt firing

Local wafer temperatures were measured using the Datapaq temperature profiler [10] both on flat (i.e. standard) and non-flat cross belt temperature profiles. In Figure 4 the actual maximum wafer temperatures, as measured in the centre of a wafer with  $\text{SiN}_x$  coating and with the test wafer in the middle of the belt, are given as a function of relative belt speed and peak zone temperature settings for the setting domain used. These iso-temperature lines were used for choosing the settings.

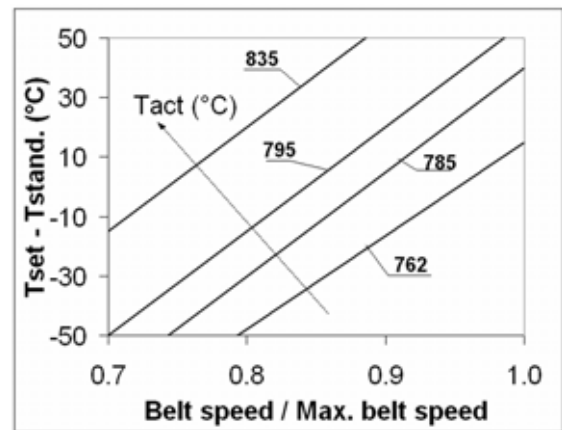


**Figure 4:** Actual wafer temperatures  $T_{\text{act}}$  as a function of furnace settings.

A new procedure was used to speed up the process of firing optimisation [11] by reducing the number of tests. The approach assumes that the front contact formation is the main factor in evaluating the performance of a paste and in achieving optimal cell results. The approach is based on relating local contact resistance to local cell temperature. To reduce the number of trials effectively, the approach uses a cross belt temperature gradient to fire a cell. This means that in one run, various locations on the cell are exposed to different temperatures. By relating the local contact resistance to the local wafer temperature, it is possible to assess if a paste leads to acceptable contact resistance values, and if so, the temperature setting for optimal firing can easily be established.

As an example of the cross belt approach, Figure 5 shows a compilation of Corescan [12] mappings for a lead free paste as function of wafer temperature. Corescan pictures for three non-flat cross belt settings have been used together with the local wafer temperatures. This paste reaches minimum contact resistance at  $T_{\text{act}} \approx 835^{\circ}\text{C}$ , being about 25 degrees higher than for the reference paste.

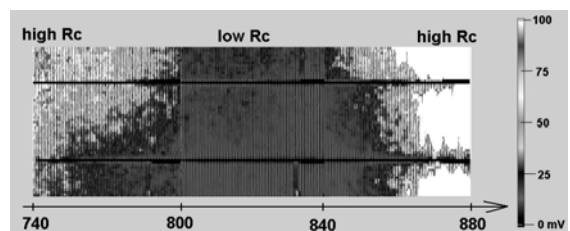


**Figure 5:** Contact resistance mapping as function of wafer temperature. The dark area represents optimal contact resistance. Note that the temperature scale is not linear.

Based on the results from the non-flat cross belt temperature testing, selected pastes have been used to make cells applying the standard flat cross belt temperature distribution.

#### 3.3 Resistance loss analysis

Slight differences in rheology can have quite an effect on the print quality in terms of width, height, and smoothness of fingers and busbars. These effects

contribute to resistance losses and therefore have great influence on fill factor and efficiency. For a full comparison of the cell results of different pastes, it is necessary to have equal line resistances and equal contact areas under the fingers. These demands are difficult to reach in case of standard processing. For the full comparison, our approach was to use double prints next to single prints and screens with various finger widths. In case of double print, with our Baccini screen printer a second print is performed exactly on the first after drying. Also, the ECN Pattern Optimiser software [13] for cell metallisation was used to establish the influence of different resistance losses of the metallisation on fill factor and efficiency.

#### 3.4 Evaluation of rear side frits and pastes

Developed rear side aluminium pastes with lead free frits were tested directly on cells with a leaded reference front side paste. Characterization included printing aspects, such as printed weight; firing aspects such as blistering, and beading; IV; resistance, and bowing of the cell.

The results for the lead free front and rear side pastes were obtained separately at the end of the project period; combination of the two pastes could not be achieved because of lack of time.

## 4 RESULTS

### 4.1 Lead free front side paste results

Our first results on lead free front side pastes were reported at the IEEE in Orlando [14]. The current results of the best cells on 156 cm<sup>2</sup> square wafers, 45 Ohm/sq. emitter are given in table I. In the processing no forming gas anneal was included.

Paste	Eta [%]	FF [%]	Jsc [mA/cm <sup>2</sup> ]	Voc [mV]
Lead free	17.0	77.2	35.9	615
Reference	17.0	77.7	35.7	614

**Table I:** Cell results comparison of lead free and leaded front side paste

With the current lead free paste contact resistances were obtained as good as the ones for the leaded reference paste. The cells were made using different screens to obtain the same printed paste weight, therefore excluding differences in line resistances. The marginally higher current for the lead free was attributed to the lower shading loss, caused by a smaller finger width. The smaller contact area then accounts for the small difference in fill factor.

No degradation of cell performance in time was detected after six months. The peel strength of soldered tab connections on lead free busbars was comparable with regards to the reference.

### 4.2 Lead free rear side paste results

The best results for the aluminium paste with lead free glass frit, as tested on 100 cm<sup>2</sup> square Cz cells, with 55-60 Ohm/sq emitter are given in table II. The cell results obtained with the lead free, fritted Al paste and a reference silver paste are competitive with Al reference paste. Moreover, the bowing in case of the reference paste was 20% higher.

Paste	Eta [%]	FF [%]	Jsc [mA/cm <sup>2</sup> ]	Voc [mV]	Bowing [ $\mu$ m]
Lead free	17.1	76.5	36.4	614	500
Reference	17.1	76.8	36.2	614	598

**Table II:** Cell results comparison of lead free and leaded rear side paste

## 5 CONCLUSIONS

Front and rear side pastes with lead free frits were successfully developed and tested. The developed model extended the insight in the complicated process of contact formation and largely contributed to the development of lead free pastes. New methods and approaches were developed to come in an effective way to frit and paste formulations, and to speed up the cumbersome optimisation of glass frits and pastes and the associated firing.

To date, best fill factor results for the lead free front and rear side pastes on Cz material are in the 77% range with efficiencies of 17%. In conclusion, the EC2Contact project has resulted in successful lead free paste formulations.

## ACKNOWLEDGEMENT

The authors would like to acknowledge Bernard Fischer and Frank Huster (UKON) for their contributions, and Ms. Boukje Ehlen (ECN) for the project management. This work was funded by the European Commission under the EC-FP5 program (EC2Contact project #ENK6-CT-2001-00560).

## REFERENCES

- [1] EC FP5 program EC2Contact project (#ENK6-CT-2001-00560), 2001
- [2] Tsoo, Y.S., et al, NREL/CP-590-23901, July 1998
- [3] de Wild-Scholten, M.J., et al, REFOCUS 5 (5), 2004, 46-49
- [4] de Wild-Scholten, M.J., et al, "Implications of European environmental legislation for photovoltaic systems", to be presented at this conference
- [5] Schubert, G., et al, Proc. 19<sup>th</sup> EPVSEC, Paris, 2004, 813-816
- [6] Schubert, G., et al, Proc. PV in Europe Conference, Rome, 2002, 343-346
- [7] Schubert, G., et al, "Silver thick film contact formation on lowly doped phosphorous emitters", to be presented at this conference
- [8] Ballif, C., et al, Appl. Phys. Lett. 82, No. 12, 2003, 1878-1880
- [9] Schubert, G., et al, Proc. 14<sup>th</sup> PVSEC, Bangkok, 2004, 441-442
- [10] Hoorstra, J., et al, Proc. PV in Europe Conf., Rome, 2002, 276-279
- [11] Hoorstra, J., et al, Proc. 19<sup>th</sup> EPVSEC, Paris, 2004, 1044-1047
- [12] Heide, A.S.H. van der, et al, Solar Energy Materials and Solar Cells 74, 2002, p. 43
- [13] Burgers, A.R., et al, Proc 26<sup>th</sup> IEEE PVSC, Anaheim, USA, 1997, 219-222
- [14] Hoorstra, J., et al, Proc. 31<sup>st</sup> IEEE PVSC, Orlando, Florida, 2005